Superstructure of Eu_4Cd_{25}: A Quasicrystal Approximant

Cesar Pay Gómez* and Sven Lidin[a]

Abstract: The quasicrystal approximant Eu_4Cd_{25}, formerly designated $EuCd_6$, was synthesized and characterized by means of single-crystal X-ray diffraction. Superstructure reflections corresponding to an *F*-centered cubic unit cell with a doubled cell-parameter relative to the *I*-centered cubic sub-cell could be observed in the diffraction data. This gives the largest cubic unit cell reported to date among binary alloys. The superstructure exhibits structural features that are found in all the RE–Cd_6 approximants as well as a further ordering between vacant/occupied Cd_8 cubes and oriented Cd_4 tetrahedra, which causes the superstructure. A reversible high-temperature phase-transition was observed at 782 K by means of DSC.

Keywords: approximants · intermetallic phases · quasicrystals · rare earths · X-ray diffraction

Introduction

The present study is part of a more extensive work aiming at resolving the ambiguities in the structural descriptions of the long-known MCd_6 phases, whereby M = rare earth element (RE) or Ca, Sr, and Y.[1] These compounds have gained renewed interest, since their classification as 1/1 approximants to the first known thermodynamically stable, binary, icosahedral quasicrystals $MCd_{5.7}$ (M = Ca and Yb).[2,3] Three prototype structures have previously been assigned to the MCd_6 family of compounds, all of which have a body-centered cubic unit cell (space group $Im\bar{3}$). However, a recent study assessing the inadequacy of this classification reveals that though all the members of the structural family are much alike, none of the members are actually isostructural with one another and the assigned prototype structures fail to accurately describe any of the members of the family.[1] The superstructure of the known compound $EuCd_6$ has long eluded attention; because of the need of good single crystal data for its identification.[4] At the time when most of the work was done in the RE–Cd systems, scientists mostly relied on powder methods as a means of structural characterization of these compounds. Among all of the MCd_6 phases characterized by means of single-crystal X-ray diffraction to date, the Eu-containing compound is the only one to indicate the presence of a superstructure resulting in a doubling of the cubic cell-parameter. Few experimental methods exist that will allow the unambiguous extraction of structural information directly from quasicrystals. Thus for the modeling of this particular class of compounds, we mostly rely on their approximants, which from a structural point of view can provide insight into local atomic arrangements that can exist in the actual quasicrystals. The title compound Eu_4Cd_{25} is of particular importance, since to a greater extent than the MCd_6 phases it gives insight into the formation and ordering mechanisms that prevail within this class of quasicrystal approximants. This information helps to elucidate the different structural variables that should be taken into account when modeling quasicrystals.

[a] C. Pay Gómez, S. Lidin
Inorganic Chemistry, Arrhenius Laboratory
Stockholm University, 106 91 Stockholm (Sweden)
Fax: (+46) 815-2187
E-mail: cesar@inorg.su.se

Experimental Section

The single crystals were obtained by high-temperature reaction of the pure elements (Eu powder 99.9% (Chempur) and Cd metal pieces from a rod of metal purified by melting). The mixture was sealed inside a stainless steel ampoule in an argon atmosphere, heated to 1173 K in a regular muffle furnace, and held at this temperature for 15 minutes to ensure the homogeneity of the melt. Subsequently the ampoule was extracted and rapidly re-inserted into another furnace already heated to 923 K, where it remained for 48 h. Finally the furnace was switched off with the sample left inside to cool down at a rate of approximately 3 K min^{-1}. The result was a homogeneous sample with an abundance of single-crystals suitable for diffraction experiments. The absence of impurities in the sample was confirmed by energy dispersive X-ray (EDX) analyses; these analyses also showed good agreement with the final composition obtained from the refinement. They were performed on a JEOL 820 scanning electron microscope (SEM) at 20 kV accelerating voltage with an Si detector LINK AN10000. Corrections were made for atomic number, absorption, and fluorescence (ZAF). A reversible phase-transition was detected by differential scanning calorimetry (DSC). These measurements were performed by using a Perkin–Elmer Pyris 1 instrument in the temperature range 673–803 K, at a heating rate of

 DOI: 10.1002/chem.200305463

5 K min^{-1}. The final measurement was made on 11.5 mg of synthesized sample that had been enclosed and hermetically sealed inside an Al ampoule in an Ar atmosphere with an empty ampoule as reference. Two empty Al ampoules were used for the base-line correction, and argon was used as a purging gas. The structural characterization was performed by means of single-crystal X-ray diffraction by using a STOE IPDS single-crystal X-ray diffractometer with a rotating anode $Mo_{K\alpha}$ X-ray source operated at 45 kV and 90 mA. The intensities of the reflections were integrated by using the STOE software, and numerical absorption corrections were applied with the programs X-RED and X-SHAPE.[5,6] The refinement of the structure was performed with the program JANA2000.[7] The electron density iso-surfaces were generated by using the program JMap3D and the images were rendered with the programs Truespace 5.2 and Diamond 2.1.[8–10] Crystmet, the metals database,[11] was used as a source for references and crystallographic information. Details of the refinement are listed in Table 1 and final atomic positions in Table 2.

Table 1. Crystallographic data from the refinement.

formula	Eu_4Cd_{25}	independent reflns	2644
M_r	3418.1	obsd reflns [$I > 3\sigma(I)$]	1812
T [K]	298	R_{int} (obsd/all)	0.0591/0.0651
space group	$Fd\bar{3}$ (no. 203)	parameters	195
a [Å]	31.8718(6)	$R1$	0.0198
V [Å^3]	32375.7(11)	$wR2(F^2)$	0.0399
Z	48	S	1.45
$F(000)$	69696	absorption correction	numerical[a]
ρ_{calcd} [g cm^{-3}]	8.4123(3)	min/max transmission	0.084/0.309
μ [mm^{-1}]	28.332	min/max $\Delta\rho$ [e Å^{-3}]	2.05/−2.28
2θ range [°]	3.3–52.1	Δ/e.s.d	0.0020

[a] From shape.

Results and Discussion

The substructure: The structures of the MCd_6 compounds can all be described with a body-centered cubic (*bcc*) arrangement of partially interpenetrating, identical cluster units (Figure 1a). The clusters are composed of four subsequent shells of atoms forming polyhedra with icosahedral symmetry. The four shells comprising the cluster unit are

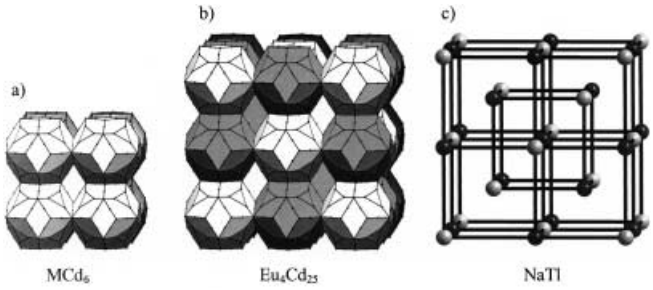

Figure 1. Cell contents of an MCd_6 phase and Eu_4Cd_{25}. In a) we see the *bcc* packing of identical, triacontahedral cluster units as it appears in an ordinary MCd_6 compound. In b) the cluster arrangement in Eu_4Cd_{25} is shown. Note that there are two different types of clusters in this image; cluster 1 (white) contains a disordered Cd_4 tetrahedron and cluster 2 (gray) contains a fully ordered Cd_4 tetrahedron; these are not visible in the image. The triangular faces on the triacontahedra indicate missing corner atoms. The cluster arrangement in Eu_4Cd_{25} is identical to the atomic arrangement in NaTl (c), and can be described by two interpenetrating NaCl-type networks with origins shifted by $^1/_4\,^1/_4\,^1/_4$.

(from the inside out): a Cd_{20} pentagonal dodecahedron followed by its dual, the M_{12} icosahedron, which alone completely defines all the positions of the M atoms in each cluster. All other atomic shells in the cluster are entirely composed of Cd atoms. The third shell is the Cd_{30} icosidodecahedron, subsequently followed by its dual, the triacontahedron that forms the outer Cd shell of the cluster. All of the above-mentioned atomic shells are shown in Figure 2b–e. Of all the atomic shells comprising the cluster unit, the triacontahedron differs from the rest in two ways. The first being that the atoms that ideally should be located at eight of the vertices with threefold symmetry are missing (this is represented by hatched triangular faces in Figure 2e). The second being that the triacontahedron not only has atoms located at its vertices, but also on its mid-edges. In spite of this fact, the polyhedron displays negligible deviation from geometrical perfection. This, in addition to the fact that the same cluster unit has been found to exist in the higher 2/1 approximants ($M_{13}Cd_{76}$ phases, M = Ca and Yb) but with other packing arrangements (*ccp* instead of *bcc*),[12,13] further authenticates the triacontahedral cluster unit as an autonomous entity suitable for the modeling of the icosahedral $MCd_{5.7}$ quasicrystals.

Table 2. Refined atomic positions of Eu_4Cd_{25}.

Atom	Wyckoff position	Occupancy	x	y	z	U_{eq} [Å^2]
Cd1t	96 g	1/3	0.2933(9)	0.2822(8)	0.2636(4)	0.079(9)
Cd2t	32e	1	0.28354(5)	0.28354(5)	0.71646(5)	0.03928(18)
Cd1d1	32e	1	0.32080(8)	0.32080(8)	0.17920(8)	0.0506(3)
Cd2d1	32e	1	0.31075(3)	0.31075(3)	0.81075(3)	0.03122(16)
Cd1d2	32e	1	0.33085(5)	0.33085(5)	0.33085(5)	0.01989(14)
Cd2d2	32e	1	0.33674(2)	0.33674(2)	0.66326(2)	0.01953(13)
Cd1d3	96 g	1	0.295502(17)	0.371031(19)	0.25159(2)	0.02414(17)
Cd2d3	96 g	1	0.295974(16)	0.872684(17)	0.24640(2)	0.01840(15)
Eu1	96 g	1	0.344570(10)	0.249030(13)	0.399681(10)	0.01272(10)
Eu2	96 g	1	0.34392(3)	0.24764(3)	0.60174(3)	0.01149(10)
Cd1id1	48f	1	0.25	0.45391(2)	0.25	0.0260(2)
Cd2id1	96 g	1	0.348037(18)	0.425550(18)	0.801398(19)	0.01726(17)
Cd1id2	96 g	1	0.349162(18)	0.422060(18)	0.306488(18)	0.01636(17)
Cd2id2	48f	1	0.25	0.45463(2)	0.75	0.0235(2)
Cd1id3	96 g	1	0.303229(19)	0.348081(19)	0.076874(19)	0.01934(18)
Cd2id3	96 g	1	0.350538(18)	0.423058(18)	0.691664(19)	0.01742(17)
Cd1	96 g	1	0.346574(14)	0.498886(18)	0.251766(16)	0.01606(12)
Cd2	96 g	1	0.325343(14)	0.202427(15)	0.499746(19)	0.01455(14)
Cd3	96 g	1	0.326358(14)	0.702612(15)	0.49921(2)	0.01471(14)
Cd1c	16c	1	0.125	0.125	0.125	0.0799(16)
Cd2c	32e	1	0.36397(6)	0.36397(6)	0.86397(6)	0.03273(17)

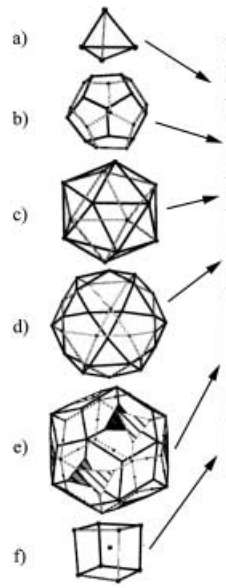

Polyhedron	Cluster 1	Cluster 2
Cd_4 Tetrahedron	Cd1t	Cd2t
Cd_{20} Dodecahedron	Cd1d1	Cd2d1
	Cd1d2	Cd2d2
	Cd1d3	Cd2d3
M_{12} Icosahedron	Eu1	Eu2
Cd_{30} Icosidodecahedron	Cd1id1	Cd2id1
	Cd1id2	Cd2id2
	Cd1id3	Cd2id3
Triacontahedron	Cd1	Cd1
	Cd2	Cd2
	Cd3	Cd3
	Cd2id1	Cd1id2
	Cd1id3	Cd2id3
Interstitial atoms in Cd_8 cubes	Cd1c	Cd2c

Figure 2. Polyhedral components of the two different cluster units and notation of the corresponding atoms. In a) we see the Cd_4 tetrahedron; in cluster 1 this polyhedron is disordered and described by the atomic position Cd1t. In b), the Cd_{20} dodecahedron composed entirely of pentagonal faces. In c), the M_{12} shell, an icosahedron containing only Eu atoms. In d), the Cd_{30} icosidodecahedron is shown. This polyhedron is composed of pentagonal and triangular faces. In e) we see the defect triacontahedron forming the external Cd shell of the cluster unit. The hatched triangular faces represent missing corner atoms. In f) a Cd_8 cube with an interstitial Cd atom is depicted. The table to the right in the Figure lists all the atomic positions that constitute every polyhedron of the two cluster units.

The three prototype structures assigned to the MCd_6 family are YCd_6, $YbCd_6$, and Ru_3Be_{17}.[14–16] These structures differ only with respect to their description of what is found inside the Cd_{20} dodecahedron. In YCd_6 and $YbCd_6$ we find a Cd_4 tetrahedron exhibiting various types of disorder, but in Ru_3Be_{17} the dodecahedron is reported to be vacant, hence the deviation from the 1:6 stoichiometry. A detailed description of the structures of the MCd_6 phases and the polyhedral shells can be found in reference [1]. That work also includes a refinement on the Eu-containing compound based solely on the substructure; the compound is referred to there as Eu_3Cd_{19}.

The superstructure: Upon longer exposure to X-rays, weak superstructure reflections giving rise to an *F*-centered cubic cell with a doubled cell parameter relative to the substructure were detected for the compound Eu_4Cd_{25}. The $(hk2)$ section of reciprocal space, obtained from the collected single-crystal data of Eu_4Cd_{25} showing both main and superstructure reflections, is shown in Figure 3a. The image has been digitally enhanced by applying a smoothing filter that brings forth the reflections without affecting their relative intensities. Figure 3b shows a section of reciprocal space perpendicular to the [850] axis; this is an approximation of the ideal pseudo-fivefold direction $[\tau 10]$. The pseudo-fivefold intensity distribution of the main reflections justifies the classification of this compound as quasicrystal approximant.

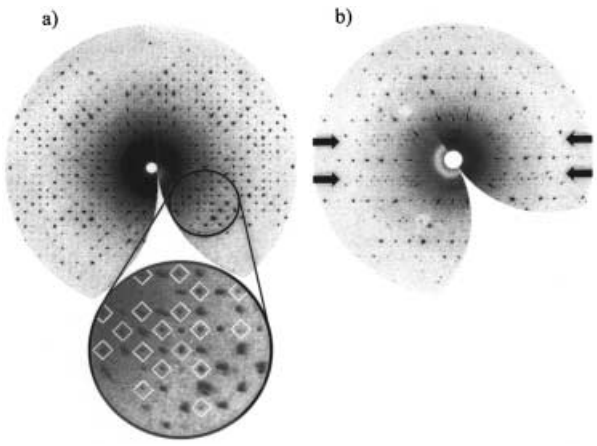

Figure 3. Sections of reciprocal space. In a) the $(hk2)$ section of Eu_4Cd_{25} is shown. In the magnified image, the superstructure reflections have been marked by white diamonds. These show how the rows of superstructure reflections are fitted in-between the rows of main reflections. In b) a section perpendicular to the pseudo-fivefold axis is shown. The image shows that the weaker superstructure reflections are aligned in horizontal rows indicated by black arrows.

Among cubic binary intermetallics, the gigantic cell with a cell parameter of 31.8718(6) Å is unprecedented, only to be rivaled by that of $NaCd_2$, which is 30.56 Å according to reference [17]. As already mentioned, the difference between the MCd_6 phases lies in the description of the disorder of the Cd_4 tetrahedron that resides within the different dodecahedral cavities or Cd_{20} dodecahedra. Of all the previously reported MCd_6-related phases, only one compound—the Ce-containing phase Ce_6Cd_{37}[18]—has a well-defined orientation of the Cd_4 tetrahedron. This is a consequence of the absence of what previously has been defined as the "type 1 disorder",[1] which is a 90° rotational disorder along the inherent twofold axis of the tetrahedron, resulting in a semi-occupied cube. All other reported MCd_6 phases that have a Cd_4 tetrahedron within their corresponding dodecahedral cavities have this type of disorder. Another type of disorder that has been observed in all the previously reported MCd_6-related phases, including Ce_6Cd_{37} and Eu_4Cd_{25}, is a triple split of the tetrahedral corner positions. This has previously been denoted the "type 2 disorder".[1] The presence of this disorder does not perturb the orientation of the Cd_4 tetrahedron significantly in the compounds Ce_6Cd_{37} and Eu_4Cd_{25}.

There is yet another difference that divides the MCd_6 family into two groups and causes deviation from the ideal 1:6 stoichiometry, thus the affected compounds are no longer "MCd_6" compounds compositionally speaking. The compositional deviations are caused by the presence of an additional Cd atom position within the cubic interstices or Cd_8 cubes that exist in all the related MCd_6, $M_{13}Cd_{76}$ and $RE_{13}(Cd/Zn)_{58}$ compounds.[1,12,13,19] Only a select few of these compounds contain atoms inside the Cd_8 interstices; among the MCd_6-related phases only those with M = Ce, Pr, or Eu are affected.[1] Every cluster unit is associated with eight Cd_8 cubes. The geometrical centers of these cubes are found in the middle of eight of the triangular faces that constitute the icosidodecahedral shells of each cluster unit; this

is where we find the interstitial Cd atoms when this position is occupied. The Cd_8 cubes are distributed within the cluster in such a way that the threefold axes of the cubic unit cell coincide with the space diagonals of all the cubes. The two corner atoms of each cube, which consequently will also be located on these threefold axes, are in fact also corner atoms of two different adjacent Cd_{20} dodecahedra. In other words the Cd_8 cubes can be regarded as bridging units between the different dodecahedral cavities belonging to adjacent cluster units. When an additional Cd atom is fitted into a Cd_8 cube, the corner atoms of the cube respond by displacing themselves farther away from this atom in order to avoid too short Cd–Cd distances. This is equivalent to saying that the adjacent Cd_{20} dodecahedra become distorted. A distortion of the dodecahedral cavities will naturally have an impact on the Cd_4 tetrahedra residing inside, affecting their relative orientation. This in turn will further distort the affected Cd_{20} dodecahedron, resulting in an infinite chain of events that propagates through the threefold axes of the cubic unit cell (Figure 4a and b). This, of course, can only occur in the MCd_6 compounds that have interstitial Cd atoms inside a certain number of Cd_8 cubes. The already mentioned Ce-containing compound has the composition Ce_6Cd_{37}. Exactly 50% of the Cd_8 cubes in this compound have an interstitial Cd atom in their central positions. This compound shows the nearest kinship to Eu_4Cd_{25}, in the sense that it is the only other cubic, MCd_6-related compound displaying a total ordering between vacant/occupied Cd_8 cubes and oriented Cd_4 tetrahedra. In Ce_6Cd_{37}, this results in a primitive unit cell instead of the usual body-centered cell into which the other MCd_6 phases conform. In Eu_4Cd_{25}, the result is a doubled face-centered cell. The only way to properly illustrate what causes the ordering in these two compounds and show how they differ from each other is to look at given segments of their corresponding threefold axes, and show the Cd_4 tetrahedra and Cd_8 cubes through which they pass. Though the chains of Cd_4 tetrahedra and Cd_8 cubes extend infinitely in the [1 1 1] and equivalent directions, these chains in these crystalline approximants are not without periodicity. Figure 4a and b show the repeating sequences encountered when traveling along threefold axes in the compounds Ce_6Cd_{37} and Eu_4Cd_{25}, respectively. In Figure 4b the atoms closest to the threefold axis have been labeled in a manner consistent with Figure 2 and Table 2. The repeating sequence is half as long in Ce_6Cd_{37} relative to that in Eu_4Cd_{25}; this can simply be explained by the fact that a Cd_8 cube being squeezed in-between two Cd_4 tetrahedra that both have their vertices directed *towards* the vertices of the cube will contract and consequently be vacant. On the other hand, a Cd_8 cube located in-between two Cd_4 tetrahedra that both have their vertices pointing *away* from the vertices of the cube will have sufficient space to allocate an additional atom in its center. The repeating sequence in Eu_4Cd_{25} contains all possible orientational combinations between Cd_4 tetrahedra and Cd_8 cubes, and furthermore shows how the Cd_8 cubes respond to these different environments. A Cd_8 cube can be located in between two tetrahedra that have: 1) both corners pointing towards the cube, 2) both corners pointing away from the cube, and 3) one corner pointing towards the cube and the other pointing away. Only combination number 1 results in a vacant Cd_8 cube; the others result in cubes with an occupied interstitial position.

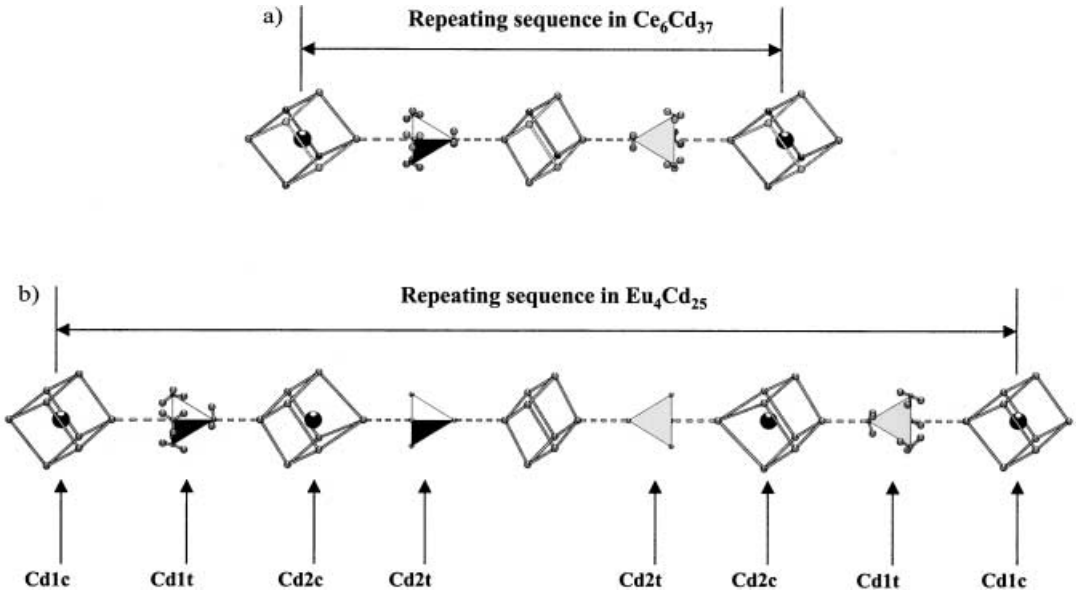

Figure 4. Repeating sequences of oriented Cd_4 tetrahedra and vacant/occupied Cd_8 cubes in the compounds Ce_6Cd_{37} (a) and Eu_4Cd_{25} (b). All atoms shown in a) and b) are Cd atoms, the atoms inside the Cd_8 cubes have been enlarged for clarity. The Cd_4 tetrahedra that are subject to the presence of the type 2 disorder are identified by the three Cd atoms that circumvent each corner. The average position of these three atoms was used to show the orientation of these tetrahedra. The first halves of the two repeating sequences are superimposed onto the second halves by operation of the inversion centers located in the middle of the vacant Cd_8 cubes in each sequence. In b), the interstitial Cd atoms and the atoms in the Cd_4 tetrahedra have been labeled. The difference between the two sequences consists of the Cd_8 cube containing the atom Cd2c and the tetrahedron composed of Cd2t, which are absent in Ce_6Cd_{37}.

As seen when comparing Figure 4a with Figure 4b, situation number 3 never occurs in Ce_6Cd_{37}. If a similar structural analysis is made emphasizing the Cd_4 tetrahedra, we find that in Eu_4Cd_{25} only the Cd_4 tetrahedra that have their vertices pointing towards occupied Cd_8 cubes are subject to the type 2 disorder. However, this is not the case in Ce_6Cd_{37}, in which all the tetrahedra possess the triple split. The atoms located in the absolute vicinity of the threefold axes are those displaying the highest degree of disorder in Eu_4Cd_{25}. Here we find the atoms with the highest temperature parameters, split positions, and the highest residual electron densities. This is a consequence of occasional variations and stacking faults in the repeating sequence seen in Figure 4b. The high degree of positional co-dependence between these atoms makes them more sensitive to defects than the other atoms in the structure. In spite of this disorder, there is nothing to indicate that Eu_4Cd_{25} is other than stoichiometric. Details of the refinement are listed in Table 1 and final atomic positions in Table 2. Actual electron density maps

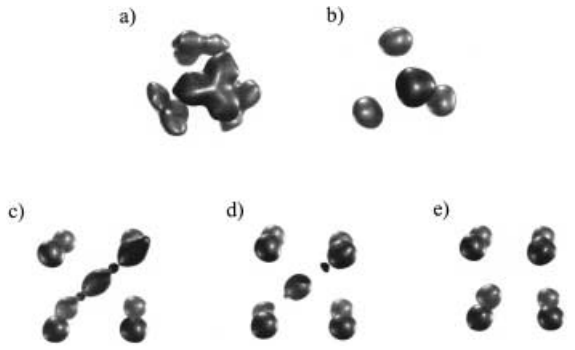

Figure 5. Electron density iso-surfaces generated from F_{obs} data at the 10 e Å^{-3} level. In a) and b), the Fourier maps of the two Cd_4 tetrahedra defined by the positions Cd1t and Cd2t respectively, are shown. The type 2 disorder (triple split) of the Cd1t position is clearly visible in a), this atomic position was refined with third order anharmonic tensors. In b) we see that the tetrahedron defined by Cd2t is fully ordered. The maps of the three different Cd_8 cubes are seen in c) to e). In c) we see the electron density distribution in the location of the cube containing the atom Cd1c. This atom displays a strong tendency to translational disorder, manifesting itself as two smaller lobes at its ends. The two corner atoms of the cube located on the threefold axis respond by elongating themselves. Instead of a split position approach, this atomic position (Cd1c) was modeled with fourth order anharmonic tensors, resulting in a much more stable refinement. In d), the Cd_8 cube containing the atom Cd2c is shown. The three atoms on the threefold axis show tendencies to translational disorder in this case as well. Finally, e) shows the vacant Cd_8 cube.

showing the electron density distributions in the locations of the two crystallographically independent Cd_4 tetrahedra and the three different Cd_8 cubes of Eu_4Cd_{25} are shown in Figure 5a–e.

The structure of Eu_4Cd_{25} may, as with all MCd_6-related phases, be described with a *bcc* packing of partially interpenetrating, triacontahedral cluster units. However, there is a significant difference between Eu_4Cd_{25} and the other MCd_6-related phases: There are *two* different cluster units that, with the exception of the mutually shared atoms in their outer triacontahedral shells, are crystallographically independent. They differ mainly in how the atoms in their corresponding Cd_4 tetrahedra are arranged. Eu_4Cd_{25} contains two independent types Cd_4 tetrahedra, one in each type of cluster unit; the electron density iso-surfaces generated from the F_{obs} data for these two types of tetrahedra are shown in Figure 5a and b. The tetrahedra described by the atomic position labeled Cd1t in Figure 2 and Table 2 show the clear presence of the type 2 disorder (triple split), while the others, described by the atomic position Cd2t are devoid of all types of disorder. This is the first case among all the MCd_6-related phases in which perfectly ordered Cd_4 tetrahedra have been observed. In the ensuing text, a cluster unit containing a tetrahedron with the type 2 disorder will be denoted "cluster 1", a cluster unit containing a perfectly ordered tetrahedron will be denoted "cluster 2". Figure 2 contains a listing of all the atoms that constitute each and every polyhedron in the two cluster types. The nomenclature for the atoms obeys the following rules: First the atom type is shown (Cd or Eu), followed by a number that indicates to which cluster the atom belongs (1 or 2). Subsequently comes a short notation indicating to which polyhedron the atom belongs (t = tetrahedron, d = dodecahedron, id = icosidodecahedron and c = Cd_8 cube), and finally a number to distinguish different atoms on the same polyhedron from each other. The atom Cd1id2, for example, is the second Cd atom in the icosidodecahedron of cluster 1. Exceptions to these rules are made for the Eu atoms that only require the first number indicating cluster belonging to be fully identified, and the triacontahedral shells that share all the atoms with adjacent clusters.

Figure 1 shows the complete structure of Eu_4Cd_{25} and also the structural difference with an ordinary MCd_6 compound composed of only one type of clusters. Figure 1c shows that the cluster arrangement in Eu_4Cd_{25} is identical to the atomic arrangement of the well-known Zintl phase NaTl,[20] which can be described as two interpenetrating NaCl networks with origins shifted by $^1/_4\,^1/_4\,^1/_4$ relative to each other.

Differential scanning calorimetry (DSC) and high-temperature measurements: A reversible phase transition was detected at 509 °C (782 K) by means of DSC (Figure 6). It was found that this transition was reversible only when the measurement was made using sealed ampoules. Another measurement made by differential thermal analysis (DTA) combined with thermogravimetric analysis (TGA) was performed with an open corundum crucible. This measurement showed the same endothermic transition at 509 °C followed by a substantial weight loss in the TGA curve. A reversible phase-transition was also reported for the related compound Ce_6Cd_{37},[18] in this case the authors suggested a model in which the transition could involve a change of the inherent disorder of the central Cd_4 tetrahedron, whereby this disorder would change from being static to being dynamic. The exact nature of the phase-transition observed for Eu_4Cd_{25} could not be ascertained from the present experiment; however, it is worth noting that the onset point for the phase transition is located at 509 °C on both heating and cooling, thus showing no evidence of a temperature hysteresis. This indicates a homogeneous (solid–solid) phase transition.

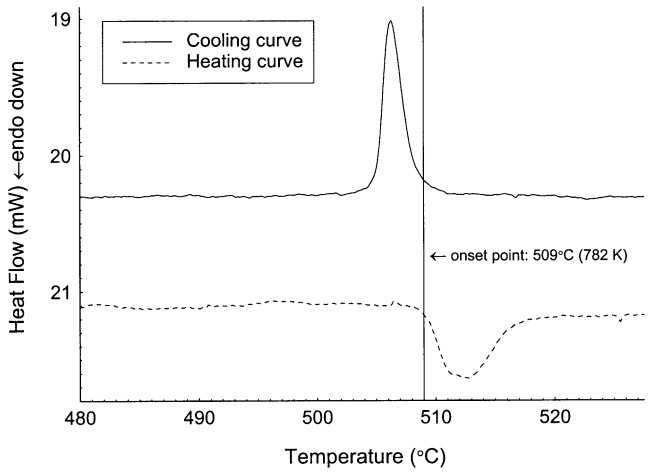

Figure 6. DSC curves for Eu_4Cd_{25}. The curves indicate the presence of a reversible phase-transition. Both heating and cooling curves indicate transitions at the same onset point, 509 °C (782 K), which is marked with the vertical line. Though the peak shape in the heating curve is somewhat more irregular; the integrated areas under the peaks of the heating and cooling curves agree very well.

Concluding remarks

The superstructure of Eu_4Cd_{25} gives valuable insight into how the ordering mechanisms that prevail in the MCd_6-related quasicrystal approximants function and propagate. It has for some time been questioned how the Cd_4 tetrahedra that break the otherwise icosahedral symmetry of the cluster unit can participate in the formation of the icosahedral $MCd_{5.7}$ quasicrystals.[3,21] The structures of Eu_4Cd_{25} and Ce_6Cd_{37} show that the Cd_4 tetrahedra, in collaboration with the Cd_8 cubes, can form the basis of higher order in these systems; whether this is a competing or cooperating driving force to quasicrystallinity is an interesting question though difficult to answer. The diffraction pattern shown in Figure 3b, however, shows that the superstructure reflections are aligned in horizontal rows that in no way contribute to the pseudo-fivefold intensity distribution displayed by the main structure reflections. We also know that any structural model taking the herein presented ordering mechanisms into account could once again only be relevant in a structure with filled Cd_8 cubes, and as far as we know, the 1/1 approximants to the $MCd_{5.7}$ quasicrystals, namely $CaCd_6$ and $YbCd_6$, have vacant Cd_8 cubes. This, however, does not necessarily mean that the Cd_8 interstices have to be vacant in the actual quasicrystals. What is the requisite for having occupied Cd_8 cubes? The answer appears to have something to do with the size of the M atoms. In order to allocate interstitial Cd atoms inside the Cd_8 cubes of an MCd_6 compound the structure needs to expand. It is, therefore, no coincidence that only the largest M atoms form compounds with occupied Cd_8 interstices. In fact, it is easy to see that these interstices start to fill when the center-to-vertex distance of the Cd_8 cubes starts to approximate the Cd–Cd distance in pure metallic Cd. In other words, the Cd_8 cubes hosting an additional Cd atom in their centers can be regarded as small fragments of metallic *bcc* Cd. The compound with M = Pr appears to be a borderline case; the center-to-vertex distance of the Cd_8 cubes in this compound is slightly shorter than the Cd–Cd distance in metallic Cd. As a consequence, this compound is the only one among the MCd_6-related phases to be nonstoichiometric, with a variable ratio of randomly distributed vacant/occupied Cd_8 cubes.[1] No MCd_6 phase containing an M atom with metallic radius smaller than that of Pr has ever been observed to contain additional Cd atoms within the Cd_8 interstices. Based on size alone, there are two more MCd_6-forming metals besides Ce, Pr, and Eu that qualify for having interstitial atoms inside the cubic interstices by being larger than Pr; these two metals are Ca and Yb. The question then arises why $CaCd_6$ and $YbCd_6$ have vacant Cd_8 cubes. We can see that when a sufficiently large M atom is inserted into an MCd_6 compound causing a uniform expansion of the structure, the newly gained space can be used in two different ways. The first is, as already mentioned, to allocate more Cd atoms inside the cubic interstices. The second is to reorient the Cd_4 tetrahedra so that their corners point more directly towards the corners of the Cd_8 cubes by minimizing the triple split, a phenomenon that would otherwise yield too short Cd–Cd distances. Why only the compounds containing Ca and Yb choose the second alternative is as puzzling as why these same two elements are the only ones to form quasicrystals when combined with Cd, though the 1/1 approximants exist in almost every RE–Cd system.

Acknowledgement

This study has been financially supported by the Swedish Natural Science Research Council and the Foundation for Strategic Research.

[1] C. Pay Gómez, S. Lidin, *Phys. Rev. B* **2003**, *68*, 024203, 1–9.
[2] J. Q. Guo, E. Abe, A. P. Tsai, *Phys. Rev. B* **2000**, *62*, R14, 605–608.
[3] A. P. Tsai, J. Q. Guo, E. Abe, H. Takakura, T. J. Sato, *Nature* **2000**, *408*, 537–538.
[4] K. H. J. Buschow, F. J. van Steenwijk, *Physica B+C* **1977**, *85*, 122–126.
[5] X-RED, STOE & Cie GmbH, Darmstadt (Germany), **1996**, v. 1.07.
[6] X-SHAPE, STOE & Cie GmbH, Darmstadt (Germany), **1996**, v. 1.01.
[7] JANA2000, V. Petøíèek, M. Dusek, Institute of Physics AVCR, Praha (Czech Republic), **2002**.
[8] JMap3D, S. Weber, NIRIM, Tsukuba (Japan), **1999**.
[9] Truespace, R. Ormandy, Caligari Corporation, Mountain View (USA), **2000**, v. 5.2.
[10] Diamond, K. Brandenburg, Crystal Impact, Bonn (Germany), **1999**, v. 2.1c.
[11] CRYSTMET search, Toth Information Systems Inc., Ottawa, Canada, **1999**, v. 1.0.
[12] C. Pay Gómez, S. Lidin, *Angew. Chem.* **2001**, *113*, 4161–4163; *Angew. Chem. Int. Ed.* **2001**, *40*, 4037–4039.
[13] C. Pay Gómez, unpublished results.
[14] A. C. Larson, D. T. Cromer, *Acta Crystallogr. Sect. B* **1971**, *27*, 1875–1879.
[15] A. Palenzona, *J. Less-Common Met.* **1971**, *25*, 367–372.
[16] D. E. Sands, Q. C. Johnson, O. H. Krikorian, K. L. Kromholtz, *Acta. Crystallogr.* **1962**, *15*, 1191.
[17] Q. B. Yang, S. Andersson, L. Stenberg, *Acta Crystallogr. Sect. B.* **1987**, *43*, 14–16.

[18] M. Armbrüster, S. Lidin, *J. Alloys Compd.* **2000**, *307*, 141 – 148.
[19] C. Pay Gómez, S. Lidin, *Solid State Sci.* **2002**, *4*, 901 – 906.
[20] E. Zintl, *Z. Phys. Chem. B* **1932**, *16*, 195-.
[21] H. Takakura, J. Guo, A. P. Tsai, *Philos. Mag. Lett.* **2001**, 81, 411 – 418.

Received: August 18, 2003
Revised: March 22, 2004
Published online: May 6, 2004

